COMMUNICATION

Check for updates

Interrogating the steric outcome during H$_2$ heterolysis: in-plane steric effects in the regioselective protonation of the PN^{3}P-pincer ligand†

Changguang Yao,[a] Tonghuan Zhang,[a,b] Chunhui Zhou[a] and Kuo-Wei Huang [iD] *[a]

H$_2$ heterolysis to generate well-defined nickel hydride-proton complexes was achieved by the 2nd generation PN^{3}P-pincer nickel platform. The regioselective protonation in the ligand framework was demonstrated for the first time to highlight the importance of in-plane hindrance during the H$_2$ splitting process.

Heterolytic splitting of H$_2$ to generate a proton (H$^+$) and hydride (H$^-$) has been considered to play a central role in H$_2$ activation catalyzed by hydrogenase enzymes,[1] which usually either contain a bimetallic core, [FeFe]/[FeNi], or a single Fe center as the active site.[1a,b] Investigations of the detailed structure of [FeFe]-hydrogenases have shown that a pendant amine base, acting as a proton relay, serves a vital role in facilitating the formation or heterolysis of H$_2$.[2] To mimic the catalysis of hydrogenases (Fig. 1A), a large number of Ni-containing models have been artificially synthesized and studied particularly by DuBois *et al.* (Fig. 1B).[3] These [Ni(P$_2^R$N$_2^{R'}$)$_2$]$^{2+}$ hydrogenase models can mediate the oxidation and reproduction of H$_2$. These systems involve either an oxidative addition of H$_2$ by directly transferring its electrons to the central Ni, or a heterolytic (asymmetric) cleavage of H$_2$ to produce the hydride-proton intermediate (Fig. 1C).[3f,h] Several investigations of heterolytic H$_2$ cleavage by nickel complexes have supported the asymmetric transition state.[3c,e,4] Heinekey and coworkers reported the first structurally well-defined nickel dihydrogen complex, in which the H$_2$ molecule cleaves heterolytically in the presence of an external triethylamine as a base (Fig. 2).[5] Caulton and co-workers showed that the cationic nickel η^2-H$_2$

complex implements H$_2$ heterolysis facilitated by the internal amine base in the ligand skeleton (Fig. 2).[4a] Bullock *et al.* reported that the oxidation rate of H$_2$ catalyzed by [Ni(P$^{Cy}_2$N$^{tBu}_2$)$_2$](BF$_4$)$_2$ increases with the decrease of the base size in the following order: NEt$_3$ < ^{t}BuNH$_2$ < ^{n}BuNH$_2$.[3m] While heterolytic H$_2$ cleavage reactions are highly relevant to enzymatic and organometallic hydrogenation processes, little is known to elucidate the influence of sterics on the protonation step. Herein, we demonstrate the metal–ligand cooperative heterolysis of H$_2$ by a [(PN^{3}P)Ni]$^+$ species with site-selective protonation to feature the importance of the in-plane steric effects (Fig. 2).

We have recently reported a new class of nickel compounds supported by a PN^{3}P-pincer ligand containing three nitrogen atoms in the ligand framework through a post-modification strategy (Fig. 3).[6] Compared with the complexes derived from the conventional 2,6-diaminopyridine based ligands,[7] these new complexes exhibited unparalleled thermal stability and distinct reactivity.[6,8] In particular, a nickel hydroxide complex (PN^{3}P)NiOH (**1**) was studied in details with respect to its strong basicity.[8b] Although hydrogenolysis of the M–OH bond to produce a M–H compound concomitant with water is a highly valuable reaction,[9] unfortunately, our Ni–OH complex **1** showed no reaction toward H$_2$ gas. This is in sharp contrast to other analogous Pd,[9] Pt[10] or Ru[11] complexes, where the H$_2$ molecule is readily cleaved by the M–OH moiety, presumably originating from the unfavorable formation of a (PN^{3}P)Ni(H$_2$)

[a]KAUST Catalysis Center and Division of Physical Sciences and Engineering, King Abdullah University of Science and Technology, Thuwal 23955-6900, Saudi Arabia. E-mail: hkw@kaust.edu.sa
[b]Lab of Computational Chemistry and Drug Design, State Key Laboratory of Chemical Oncogenomics, Peking University Shenzhen Graduate School, Shenzhen 518055, China
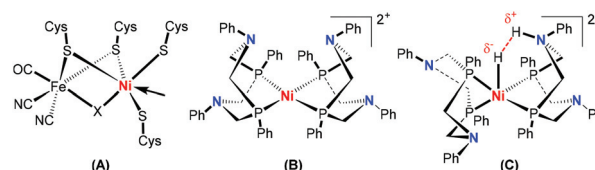
Fig. 1 Structures of hydrogenases and nickel mimics. (A) [NiFe] hydrogenase; (B) Ni hydrogenase mimic; (C) proposed transition state for production of H$_2$ catalyzed by (B).
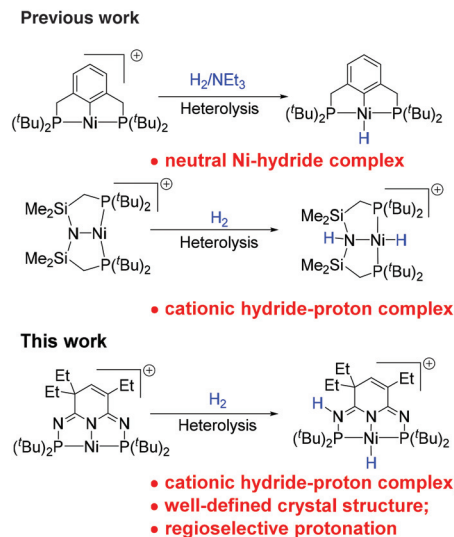
Fig. 2 Heterolysis of H$_2$ by cationic pincer nickel complexes.
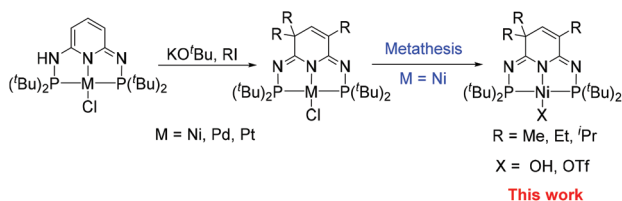
Fig. 3 Synthesis of 2nd PN^{3}P-pincer compounds through ligand post-modification strategy.

Fig. 4 Molecular structures of complexes **3**$^+$, **[5a]**$^+$ and **[7b]**$^+$. Thermal ellipsoids are shown at the 30% probability level; hydrogen atoms except Ni–H and N–H moieties are omitted for clarity. Selected bond lengths [Å] and angles [°]: for **3**$^+$: Ni(1)–N(1) 1.9015(11), Ni(1)–P(1) 2.1407(4), Ni(1)–P(2) 2.1401(4), Ni(1)–H(1) 1.351, N(2)–H(2) 0.85(1); N(1)–Ni(1)–H(1) 178.16, H(1)–Ni(1)–P(1) 91.33, H(1)–Ni(1)–P(2) 96.83, P(1)–Ni(1)–P(2) 171.776(15). For **[5a]**$^+$: Ni(1)–N(1) 1.9017(7), Ni(1)–P(1) 2.1348(3), Ni(1)–P(2) 2.1300(3), Ni(1)–H(1) 1.374, N(2)–H(2) 0.863; N(1)–Ni(1)–H(1) 178.29, H(1)–Ni(1)–P(1) 95.05, H(1)–Ni(1)–P(2) 92.98, P(1)–Ni(1)–P(2) 171.738(9). For **[7b]**$^+$: Ni(1)–N(1) 1.9022(14), Ni(1)–P(1) 2.1461(5), Ni(1)–P(2) 2.1431(5), Ni(1)–H(1) 1.37(3), N(3)–H(3N) 0.86(3); N(1)–Ni(1)–H(1) 178.3(12), H(1)–Ni(1)–P(1) 94.7(12), H(1)–Ni(1)–P(2) 93.9(12), P(1)–Ni(1)–P(2) 171.382(19).

Scheme 1 Synthesis and H$_2$ heterolysis of complex **2**.

intermediate.[4a] Caulton and co-workers have reported that a free coordination site for H$_2$ is important for the heterolysis to proceed in the pincer-type nickel compound.[4a] Consistent with their viewpoint, when one equivalent of B(C$_6$F$_5$)$_3$ was introduced to the C$_6$D$_6$ solution of **1**, the resulting borane adduct (PN^{3}P)Ni(OH)B(C$_6$F$_5$)$_3$ (**2**) could undergo the hydrogenolysis reaction. This is likely attributed to the property of anionic [(OH)B(C$_6$F$_5$)$_3$]$^-$ as a better leaving group than the OH group. However, differently from what was reported by the groups Peters[12] and Limberg,[4b] the [(PN^{3}P)Ni(H$_2$)]$^+$ intermediate was not observed.[4a,13] The hydrogenolysis reaction occurred immediately after the H$_2$ was introduced into **2**, as corroborated by the rapid color change from brown to light yellow. The ^{31}P{^{1}H} NMR showed significant downfield chemical shifts, in comparison with those from **2** (δ 103.5 and 103.2 ppm), with two sets of peaks observed at δ 147.5 and 144.9 ppm. The successful heterolysis of H$_2$ to generate a proton and a hydride was further validated by the ^{1}H NMR with a doublet of doublet peak at δ −16.20 ppm for the hydride and a signal at δ 9.41 ppm for the proton. The identity of product **3** was confirmed by X-ray crystallography (Fig. 4). Complex **3** consists of an anion [(OH)B(C$_6$F$_5$)$_3$]$^-$ and a cation [(PN^{3}HP)Ni(H)]$^+$ in which the H$^-$ and H$^+$ derived from the splitting of H$_2$ bond to the nickel center and one of the nitrogen atoms, respectively (Scheme 1). Although various experiments

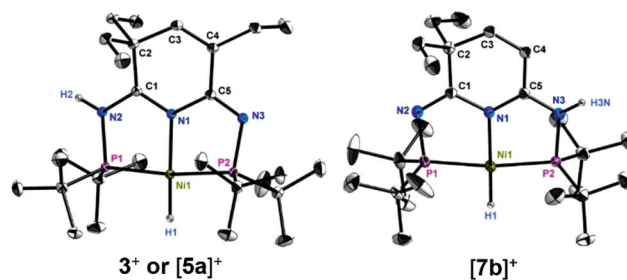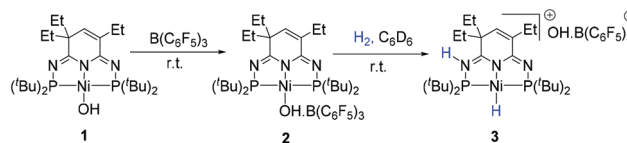on H$_2$ heterolysis catalyzed by nickel compounds have been reported, to our knowledge, no well-defined nickel hydride-proton intermediate was obtained.

In order to further verify the importance of the leaving ability of ancillary ligand, we prepared a similar complex (**4**), (PN^{3}P)NiOTf, containing a slightly stronger coordinating group, OTf, as the promoter of H$_2$ heterolysis. The comparison of the crystal structures of **2** and **4** clearly showed that the length of the Ni–O bond (1.9169(11) Å) in complex **4** is shorter than that (2.0258(15) Å) in complex **2**, suggesting that the leaving ability of (OH)B(C$_6$F$_5$)$_3$ moiety is higher than that of the OTf group. Indeed, no reaction occurred for complex **4** in the presence of H$_2$ at room temperature over 12 h. Only upon heating at 50 °C, a new product, **5a**, was slowly formed. These results suggest that the displacement of OTf by H$_2$ at an elevated temperature to generate [(PN^{3}P)Ni(H$_2$)]$^+$ may play a vital role in promoting the activation of H$_2$. The ^{1}H NMR also shows protic and hydride signals at δ 10.16 and −16.19 ppm, respectively, similar to those in complex **3**. The X-ray diffraction analysis revealed the structure of **5a** to be [(PN^{3}HP)Ni(H)]$^+$[OTf]$^-$ (Fig. 4).

Both NMR and crystal data suggested that the proton from H$_2$ heterolysis was transferred into one of the side arm nitrogen atoms of the PN^{3}P ligand (Fig. 4). Caulton and co-workers have demonstrated that nitrogen atoms could potentially serve

as a base to facilitate H_2 heterolysis.[4a] As our ligand framework contains three nitrogen atoms, in principle there are three possible protonated products formed in this system (Fig. 5). 2D NOESY experiments were conducted to determine the structure of the Ni–H cation. The cross peak at 2.89/10.16 ppm was attributed to the correlation of the N*H* proton and the methylene protons of the two ethyl groups at the same side of the ligand (Fig. S10† for complex **5a**). Likewise, the correlation of the N*H* proton and those of two equivalent *t*Bu groups could also be observed at the position of 1.29/10.16 ppm, further suggesting that the proton was selectively added to one N atom (**Ni1**$_{left}$), consistent with qualitative DFT calculations (Fig. 5). The counterpart **Ni1**$_{right}$ with the proton connecting to the N atom on the other side was found to be higher in energy. The relative Gibbs free energy of other structures **Ni1**$_{H2}$, before H_2 splitting, and **Ni1**$_{mid}$ were both found to be extremely unfavorable, indicative of the thermodynamic preference of the H_2 cleavage process.

The selective protonation of the nitrogen atom may originate from the different electronic and/or steric effects on the nitrogen atoms. To further rationalize the selectivity, an analogous nickel triflate complex (**6**) containing only two ethyl groups on the PN^{3}P framework was prepared. Interestingly, when complex **6** was used, both N side arms could be protonated to give a mixture of **7a** and **7b** in a ratio of approx. 1 : 6 (Scheme 3). The major product **7b** suggests that the steric effect is likely the dominating factor of the observed selectivity in the protonation step (Fig. 4), since **7a** should experience similar electronic effects as **5a**. This argument is further supported by very similar atomic charges from NPA of the two nitrogen sites in **4** ($q(N2) = -0.616$; $q(N3) = -0.627$). Analyzing

the molecular structure of **5a**, we notice that the diethyl groups are both out of the plane of the central heterocyclic ring, but the monoethyl group is in the plane, strongly indicating that the selectivity is caused by the in-plane hindrance. To further support this argument, two analogous complexes (**8** and **10**) were prepared *via* replacing the Et groups by Me and *i*Pr groups and employed to conduct the heterolytic splitting of H_2. It was found that the selectivity indeed remained the same (Scheme 2). The structures of **9a** and **11a** were also characterized by NMR and single crystal X-ray diffraction (Fig. 6). The distances between H and Me in **9a** (H2–C6: 2.785 Å; H2–C7: 2.892 Å) are longer than those in **9b** (H3A–C8: 2.505 Å), in agreement with the observation that protonation of the dimethyl side is more feasible (Fig. 7). When NMR experi-
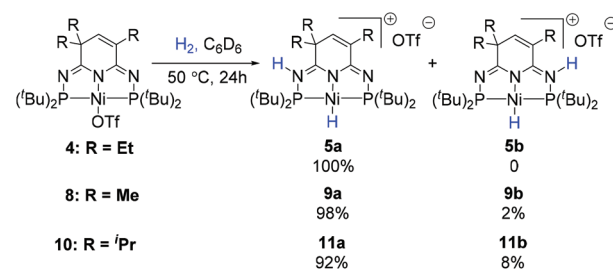
Scheme 2 Heterolysis of H_2 by [Ni-OTf] complexes.
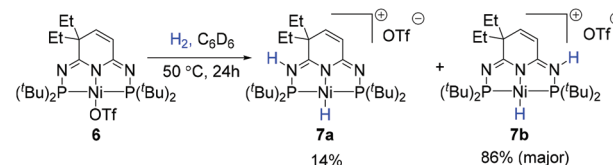
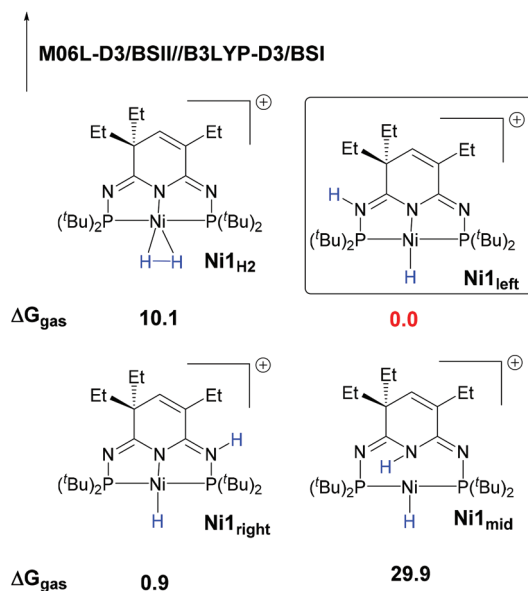**Scheme 3** Heterolysis of H_2 by complex **6**.

Fig. 5 Structures of the probable intermediates and protonated products with relative Gibbs free energy data (the energetics in the first and second lines represent the energies in gas phase and in the experimental solvent (benzene) phase, respectively).
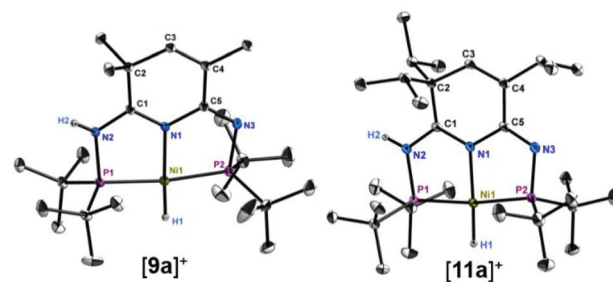
Fig. 6 Molecular structures of complexes [**9a**]$^+$ and [**11a**]$^+$. Thermal ellipsoids are shown at the 30% probability level; hydrogen atoms except Ni–H and N–H moieties are omitted for clarity. Selected bond lengths [Å] and angles [°]: for [**9a**]$^+$: Ni(1)−N(1) 1.9037(11), Ni(1)−P(1) 2.1376(5), Ni(1)−P(2) 2.1379(5), Ni(1)−H(1) 1.28(3), N(2)−H(2) 0.79(2); N(1)−Ni(1)−H(1) 177.645, H(1)−Ni(1)−P(1) 95.299, H(1)−Ni(1)−P(2) 92.700, P(1)−Ni(1)−P(2) 171.994(16). For [**11a**]$^+$: Ni(1)−N(1) 1.908(2), Ni(1)−P(1) 2.1229(7), Ni(1)−P(2) 2.1268(8), Ni(1)−H(1) 1.368, N(2)−H(2) 0.861; N(1)−Ni(1)−H(1) 176.323, H(1)−Ni(1)−P(1) 92.226, H(1)−Ni(1)−P(2) 95.120, P(1)−Ni(1)−P(2) 172.642.
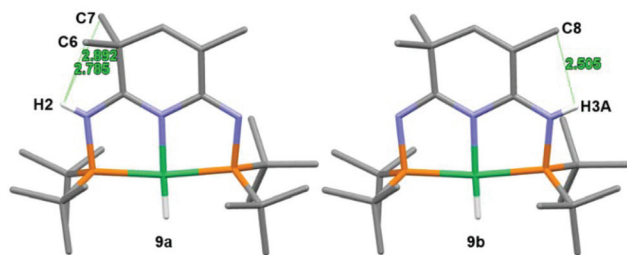
Fig. 7 The distances between H and Me in **9a** and **9b**.

ments were conducted at an elevated temperature (110 °C), the rations of **5a**/**5b** and **11a**/**11b** changed (Fig. S33 and S35†), indicating that these complexes are interchangeable. These observations suggest that these regioselective products are likely the results of thermodynamic preference driven by the in-plane hindrance between the protonated N–H arm and the H or alkyl group at the sp^2 carbon of the ring.

In summary, we have demonstrated the importance of the leaving ability of coordinated anion for the H_2 heterolysis process in the planar pincer geometry by comparing the effects of the $(OH)B(C_6F_5)_3$ and the OTf moieties. We also presented a unique model for interrogating the in-plane interactions. Using two different 2nd generation PN^3P-pincer nickel compounds (**4** and **6**), the H_2 heterolysis and regioselective protonation of the in-plane less hindered nitrogen atoms in the ligand framework was observed. Together with both DFT calculations and control experiments, the significance of the steric factor was confirmed.

Conflicts of interest

There are no conflicts to declare.

Acknowledgements

Notes and references

1 (a) C. Tard and C. J. Pickett, *Chem. Rev.*, 2009, **109**, 2245–2274; (b) W. Lubitz, H. Ogata, O. Rüdiger and E. Reijerse, *Chem. Rev.*, 2014, **114**, 4081–4148; (c) M. Winkler, M. Senger, J. Duan, J. Esselborn, F. Wittkamp, E. Hofmann, U.-P. Apfel, S. T. Stripp and T. Happe, *Nat. Commun.*, 2017, **8**, 16115; (d) M. Senger, K. Laun, F. Wittkamp, J. Duan, M. Haumann, T. Happe, M. Winkler, U.-P. Apfel and S. T. Stripp, *Angew. Chem., Int. Ed.*, 2017, **56**, 16503–16506.

2 M. R. DuBois and D. L. DuBois, *Chem. Soc. Rev.*, 2009, **38**, 62–72.

3 (a) C. J. Curtis, A. Miedaner, R. Ciancanelli, W. W. Ellis, B. C. Noll, M. Rakowski DuBois and D. L. DuBois, *Inorg.*

Chem., 2003, **42**, 216–227; (b) A. D. Wilson, R. H. Newell, M. J. McNevin, J. T. Muckerman, M. Rakowski DuBois and D. L. DuBois, *J. Am. Chem. Soc.*, 2006, **128**, 358–366; (c) A. D. Wilson, R. K. Shoemaker, A. Miedaner, J. T. Muckerman, D. L. DuBois and M. R. DuBois, *Proc. Natl. Acad. Sci. U. S. A.*, 2007, **104**, 6951–6956; (d) M. R. DuBois and D. L. DuBois, *C. R. Chim.*, 2008, **11**, 805–817; (e) J. Y. Yang, R. M. Bullock, W. J. Shaw, B. Twamley, K. Fraze, M. R. DuBois and D. L. DuBois, *J. Am. Chem. Soc.*, 2009, **131**, 5935–5945; (f) A. Kachmar, V. Vetere, P. Maldivi and A. A. Franco, *J. Phys. Chem. A*, 2010, **114**, 11861–11867; (g) J. Y. Yang, S. Chen, W. G. Dougherty, W. S. Kassel, R. M. Bullock, D. L. DuBois, S. Raugei, R. Rousseau, M. Dupuis and M. R. DuBois, *Chem. Commun.*, 2010, **46**, 8618–8620; (h) M. Dupuis, S. Chen, S. Raugei, D. L. DuBois and R. M. Bullock, *J. Phys. Chem. A*, 2011, **115**, 4861–4865; (i) M. L. Helm, M. P. Stewart, R. M. Bullock, M. R. DuBois and D. L. DuBois, *Science*, 2011, **333**, 863–866; (j) T. Liu, S. Chen, M. J. O'Hagan, M. Rakowski DuBois, R. M. Bullock and D. L. DuBois, *J. Am. Chem. Soc.*, 2012, **134**, 6257–6272; (k) S. E. Smith, J. Y. Yang, D. L. DuBois and R. M. Bullock, *Angew. Chem., Int. Ed.*, 2012, **51**, 3152–3155; (l) S. Wiese, U. J. Kilgore, D. L. DuBois and R. M. Bullock, *ACS Catal.*, 2012, **2**, 720–727; (m) J. Y. Yang, S. E. Smith, T. Liu, W. G. Dougherty, W. A. Hoffert, W. S. Kassel, M. R. DuBois, D. L. DuBois and R. M. Bullock, *J. Am. Chem. Soc.*, 2013, **135**, 9700–9712; (n) A. Dutta, D. L. DuBois, J. A. S. Roberts and W. J. Shaw, *Proc. Natl. Acad. Sci. U. S. A.*, 2014, **111**, 16286–16291; (o) N. Priyadarshani, A. Dutta, B. Ginovska, G. W. Buchko, M. O'Hagan, S. Raugei and W. J. Shaw, *ACS Catal.*, 2016, **6**, 6037–6049; (p) E. B. Hulley, K. D. Welch, A. M. Appel, D. L. DuBois and R. M. Bullock, *J. Am. Chem. Soc.*, 2013, **135**, 11736–11739.

4 (a) T. He, N. P. Tsvetkov, J. G. Andino, X. F. Gao, B. C. Fullmer and K. G. Caulton, *J. Am. Chem. Soc.*, 2010, **132**, 910–911; (b) H. Gehring, R. Metzinger, C. Herwig, J. Intemann, S. Harder and C. Limberg, *Chem. – Eur. J.*, 2013, **19**, 1629–1636.

5 S. J. Connelly, A. C. Zimmerman, W. Kaminsky and D. M. Heinekey, *Chem. – Eur. J.*, 2012, **18**, 15932–15934.

6 (a) X. F. Wang, L. F. Yao, Y. P. Pan and K.-W. Huang, *J. Organomet. Chem.*, 2017, **845**, 25–29; (b) M.-H. Huang, J. Hu and K.-W. Huang, *J. Chin. Chem. Soc.*, 2018, **65**, 60–64.

7 (a) H. Li, B. Zheng and K.-W. Huang, *Coord. Chem. Rev.*, 2015, **293**, 116–138; (b) H. Li, T. P. Gonçalves, D. Lupp and K.-W. Huang, *ACS Catal.*, 2019, **9**, 1619–1629; (c) T. P. Gonçalves and K.-W. Huang, *J. Am. Chem. Soc.*, 2017, **139**, 13442–13449; (d) H. Li, T. P. Gonçalves, Q. Zhao, D. Gong, Z. Lai, Z. Wang, J. Zheng and K.-W. Huang, *Chem. Commun.*, 2018, **54**, 11395–11398; (e) H. Li, T. P. Gonçalves, J. Hu, Q. Zhao, D. Gong, Z. Lai, Z. Wang, J. Zheng and K.-W. Huang, *J. Org. Chem.*, 2018, **83**, 14969–14977.

8 (*a*) C. Yao, X. Wang and K.-W. Huang, *Chem. Commun.*, 2018, **54**, 3940–3943; (*b*) C. Yao, P. Chakraborty, E. Aresu, H. Li, C. Guan, C. Zhou, L.-C. Liang and K.-W. Huang, *Dalton Trans.*, 2018, **47**, 15997–16360.

9 G. R. Fulmer, R. P. Muller, R. A. Kemp and K. I. Goldberg, *J. Am. Chem. Soc.*, 2009, **131**, 1346–1347.

10 T. T. Wenzel, in *Stud. Surf. Sci. Catal*, ed. L. I. Simándi, Elsevier, 1991, vol. 66, pp. 545–554.

11 T. Matsumoto, Y. Nakaya, N. Itakura and K. Tatsumi, *J. Am. Chem. Soc.*, 2008, **130**, 2458–2459.

12 C. Tsay and J. C. Peters, *Chem. Sci.*, 2012, **3**, 1313–1318.

13 (*a*) T. Chen, H. Li, S. Qu, B. Zheng, L. He, Z. Lai, Z.-X. Wang and K.-W. Huang, *Organometallics*, 2014, **33**, 4152–4155; (*b*) Y. Wang, B. Zheng, Y. P. Pan, C. L. Pan, L. P. He and K.-W. Huang, *Dalton Trans.*, 2015, **44**, 15111–15115.